Magnetic pinching of fast electron transport in solid targets diagnosed using measurements of proton acceleration

Contact p.mckenna@phys.strath.ac.uk

X. H. Yuan*, M. N. Quinn, D. C. Carroll, P. Gallegos# and P. McKenna
SUPA Department of Physics, University of Strathclyde, Glasgow G4 0NG, UK
* also at State Key Laboratory of Transient Optics and Photonics, Xi'an Institute of Optics and Precision Mechanics, CAS, Xi'an 710119, China
# also at Central Laser Facility, STFC, Rutherford Appleton Laboratory

A. P. L. Robinson, R. J. Clarke and D. Neely
Central Laser Facility, STFC, Rutherford Appleton Laboratory, HSIC, Didcot, Oxon OX11 0QX, UK

R. G. Evans
The Blackett Laboratory, Imperial College London, London SW7 2 BZ, UK
(also at Central Laser Facility, STFC, Rutherford Appleton Laboratory)

K. Quinn, L. Romagnani, G. Sarri, P. A. Wilson and M. Borghesi
Department of Physics and Astronomy, Queen's University of Belfast, Belfast BT7 1NN, UK

L. Lancia and J. Fuchs
LULI, École Polytechnique-Université Paris VI, 91128 Palaiseau, France

Introduction

The transport of fast electrons generated in the interaction of a relativistically intense laser pulse with overdense plasma is of fundamental importance for the fast ignition (FI) approach to inertial fusion energy[1], and plays a crucial role in the optimization of high power laser-driven ion sources[2]. A requirement for FI, is that the fast electrons are efficiently transported over hundreds of micrometers and deliver energy to the compressed fuel. The divergence of the fast electron beam is important, as it defines the size of the electron source (for a given fuel pellet size) and the separation between the source and the fuel. Simulations show that if the divergence of the fast electron beam is ≥50° a laser drive energy of ~150 kJ is required[3], which would make this approach to FI impractical. Recent experiments employing K_α imaging in metallic targets of thickness <100 μm reveals a significant beam divergence which is found to increase with increasing laser intensity (half angle ~27° for 5×10^{20} Wcm^{-2})[4].

The fast electrons generated at the front irradiated surface of a solid target foil propagate through the target and produce an electrostatic sheath field at the rear non-irradiated surface. This field has strength on the order of TV/m, and ionizes the atoms at the rear surface resulting in the acceleration of ions to multi-MeV energies. This mechanism is called Target Normal Sheath Acceleration (TNSA)[2]. The properties of the ion beam are sensitive to the electron sheath. Spatial and energy resolved measurements of the accelerated ions provide a diagnostic of the spatial profile of the electron sheath at the target rear surface, and hence the electron transport through the target.

We report on a radically new approach to measuring the effect of magnetic collimation of the fast electron beam in metallic targets based on measurements of proton emission. The results show that some degree of collimation occurs due to self-generation of B-field.

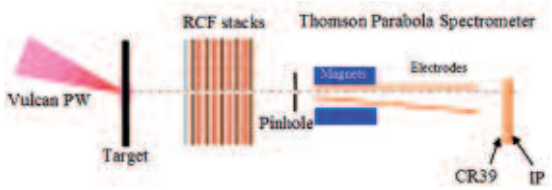

Figure 1. Experimental set-up showing ion diagnostics.

Experiment

The experiment was carried out using the Vulcan petawatt laser facility, delivering pulses with energy of ~280 J on target, in 700 fs (FWHM), at 1.053 μm wavelength. The p-polarized laser pulses were focused, with an f /3 off-axis parabolic mirror, onto a solid target at an incident angle of 13° from the target normal. The focus spot was 6 μm diameter (FWHM), which produced a peak intensity of $\sim6\times10^{20}$ W/cm^2. Planar Al targets with size 3 mm × 7 mm and thickness varying from 25 μm up to 1.4 mm, were used. The main diagnostic for multi-MeV proton emission was a passive radiochromic film (RCF) stack, types HD-810 and MD-V2-55, placed 50 mm behind the target foil in the normal direction. This measures the proton beam spatial intensity distribution at discrete energies corresponding to the deposited Bragg peaks. The minimum measurable proton energy was 6.5 MeV in the general design. From the RCF stack, measurements of the maximum proton energy, proton spectra (thus the laser-to-proton energy conversion efficiency) and proton beam divergence are obtained. A slot was machined into the RCF stack so that a sight to the target was possible for a Thomson parabola spectrometer (TP-Spec). The TP-Spec, also positioned along the target normal, was used to measure the energy and charge-to-mass distributions of the emitted ions. A piece of CR-39 nuclear track detector, backed with a Fuji-film image plate (IP), was used to record proton and heavier ion tracks. The

measurement of efficient heavy ion emission from thick targets confirms that TNSA is the dominant ion acceleration mechanism for the laser and target parameters of the experiment. Figure 1 shows a schematic of the experimental set up.

Results

Two properties of the beam of accelerated protons, the maximum energy (E_{max}) and the laser-to-proton energy conversion efficiency (η) are plotted in figure 2 as a function of target thickness (L). The measurements of E_{max} using the RCF stack and TP-Spec are in good agreement. The near-linear decrease in E_{max} with L is surprising. By a simple argument, the fast electron density in the sheath is inversely proportional to the sheath area and should therefore decrease with L^2.

To investigate this further, we calculate the expected E_{max} as a function of L. The maximum achievable proton energy can be analytically estimated, using Mora's isothermal plasma expansion model [5], as $E_{max} \approx 2k_BT[\ln(\tau+(\tau^2+1)^{1/2})]^2$, where k_BT is the temperature of fast electrons and $\tau = 0.43t_a\omega_p$, t_a is the acceleration time determined by the pulse duration and ω_p is the plasma frequency proportional to $n_e^{1/2}$ (n_e is the fast electron density). The parameters t_a and k_BT_e are assumed to remain constant with increasing L. This is justified on the basis of electron transport results reported separately [6]. The fast electron density is determined by assuming ballistic transport of fast electrons through the target with a fixed angle of divergence. The resulting calculated E_{max} variation with L is shown in Fig 2(a) for three half angles of divergence: 10°, 16° (as inferred from coherent transition radiation measurements [7]) and 27° (as inferred from K_α measurements [4]). Fig 2(a) also shows the plasma expansion calculations adjusted to take account of the reduced n_e at the rear surface due to scattering within the target. These scattering corrections are based on results from simulations using the Monte Carlo code GEANT4 [8], and reduce the expected E_{max}.

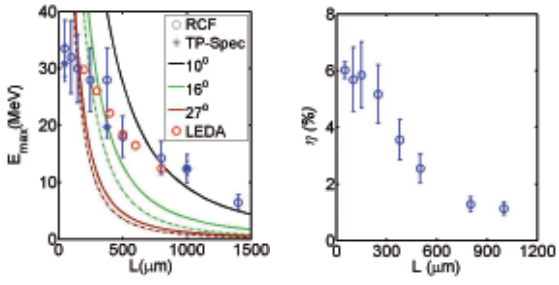

Figure 2. (a) Maximum proton energy (E_{max}) as a function of target thickness (L). Experimental results are from RCF stack (blue open circle) and Thomson parabola spectrometer (TP-Spec, blue star). The error bars include the variation over multiple shots and energy resolution for RCF stack design. Solid lines correspond to plasma expansion model calculations assuming ballistic transport of the electrons at given divergence angles. The corresponding dashed lines include scattering. Simulation results using LEDA code is shown in red open circle. (b) Laser to proton energy conversion efficiency (η) with target thickness (L) calculated from RCF stack measurement.

It is clear from figure 2(a) that the measured proton energies differ significantly from that expected due to ballistic transport of the fast electrons through the targets. The expected half angle of divergence for the laser and target parameters is 27°, as determined from K_α measurements [4]. The measured proton E_{max} is consistent with this at L~200 μm, but the divergence angle is found to decrease significantly for larger L.

An analytical model of the evolution of the electron sheath and resulting ion front has been developed to determine the initial sheath size as a function of L, based on a fit of the calculated proton beam divergence as a function of energy with the measured values. This model will be described elsewhere [6]. The results show a non-linear increase in the sheath size with L.

To explain the observed reduction in the electron beam divergence in thick targets we need to invoke the pinching effect of the azimuthal magnetic field resistively self-generated by the fast electron beam. The degree of the collimation produced by this field was theoretically investigated by Bell and Kingham [9]. The B-field growth is governed by the electron beam and target material properties and should be independent of target thickness. However, refluxing of the fast electrons within thin targets (reflected at the sheaths formed at both surfaces) leads to counter-streaming fast electrons which locally cancel out the net forward fast electron current, terminating the growth of the self-generated B-field. For a target with L=200 μm, for example, electrons moving at c will be reflected from the rear and returned to the front surface, where the magnetic field is strongest, in ~1.3 ps. The decrease in beam divergence with increasing L is likely to result from an increased effectiveness of the self-generated magnetic field due to the decreasing influence of electron refluxing on the field generation.

Simulations

To investigate this hypothesis we performed fast electron transport simulations using the 2D hybrid Vlasov-Fokker-Planck code LEDA [10]. The input parameters were chosen to match the experimental conditions. The laser intensity was set to 5×10^{20} W/cm^2 and the pulse duration equal to 700 fs. The half angle of injection of the electrons was 24°. The initial ion background temperature is 1 eV. A uniform spatial grid, 1 μm per cell, is used for all the simulation runs. Simulation runs were performed as a function of target thickness from L=80 μm to L=800 μm. All other parameters were identical.

Figure 3 shows example simulation outputs at 950 fs after the start of the laser pulse. The magnetic field (B_z) distributions and fast electron density (n_e) are plotted for 300 μm and 80 μm. By 950 fs, the fast electrons have transversed the 80 μm target three times, but have not yet reached the rear of the 300 μm target. Large differences are observed in the electron density and magnetic field distributions. The self-generated azimuthal B-field is clearly observed in the L=300 μm target and extends ~100 μm from the electron source, figure 3 (a). However, the B-field is considerably fragmented for thinner case, figure 3 (b), which destroys the collimating effect.

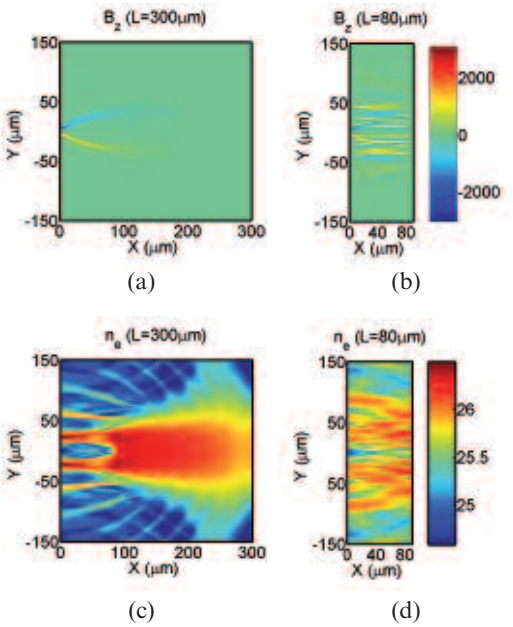

Figure 3. The magnetic flux density (in Tesla) for target thickness equal to (a) 300 μm and (b) 80 μm, at 950 fs after the laser pulse interaction (at x=0, y=150). $\log_{10}$ of the electron density (m^{-3}) that corresponds to (a) is shown in (c) and that of (b) is shown in (d).

The average fast-electron density, n_e, on-axis (y=0) at the rear surface of the target as a function of L was extracted from the simulation results and used as an input to the plasma expansion formulae (with the same assumptions discussed above) to calculate E_{max}. The results are found to be in excellent agreement with the experimental results, as shown in Fig. 2 (a).

Conclusions

Measurements of proton emission have been used to investigate fast electron transport in thick solid target (up to 1.4 mm) at an intensity of 6×10^{20} W/cm^2. This diagnostic technique has an advantage over other techniques in that it is directly sensitive to the fast electron density in the MeV range at the target rear surface. We measure a clear departure from the model of ballistic transport of the electrons through the target at a fixed divergence angle. The measurements are explained by the pinching effect of the self-generated magnetic field. The field is more effective in thicker targets due to the absence of electron refluxing within the target. A more detailed presentation of the results will be made in a future publication [6].

Acknowledgements

The authors would like to acknowledge the scientific and technical support of the staff at the Central Laser Facility. The authors also thank Dr. R. Martin for his help in using a computer cluster at the University of Strathclyde, and Dr. J. Melone and Ms S. Cipiccia for their assistance in running Geant4 simulations. This work is funded by ESPRC Grant No. EP/E048668/1 and the EU COST P-14 Action.

References

1. M. Tabak *et al.*, *Phys. Plasmas* **1**, 1626 (1994).
2. S. C. Wilks *et al.*, *Phys. Plasmas* **8**, 542 (2001).
3. HiPER technical report (www.hiper-laser.org)
4. J. S. Green *et al.*, *Phys. Rev. Lett*. **100**, 015003 (2008).
5. P. Mora, *Phys. Rev. Lett*. **90**, 185002 (2003).
6. X. H. Yuan *et al.*, in preparation
7. M. Storm *et al.*, *Phys. Rev. Lett*. **102**, 235004 (2009).
8. S. Agostinelli *et al.*, *Nucl. Instr. and Meth. A* **506**, 250 (2003).
9. A. R. Bell and R. J. Kingham, *Phys. Rev. Lett*. **91**, 035003 (2003).
10. A. P. L. Robinson and M. Sherlock, *Phys. Plasmas* **14**, 083105 (2007).